

Note on the mineral texture and chemistry of the eastern Bushveld Complex

Sotaro Baba¹, Tomokazu Hokada¹, Tetsu Saitoh², Yoshikuni Hiroi³, Kazuyuki Shiraishi¹, Makoto Arima² and Robin E. Harmer⁴

¹*Department of Crustal Studies, National Institute of Polar Research, Kaga 1-chome, Itabashi-ku, Tokyo 173-8515*

²*Geological Institute, Yokohama National University, 79-2, Tokiwadai, Hodogaya-ku, Yokohama 240-8501*

³*Department of Geology, Faculty of Science, Chiba University, 1-33, Yayoi-cho, Chiba 263-8522*

⁴*Council for Geoscience, Private Bag X112, Pretoria 0001, South Africa*

Abstract: Preliminary petrological study was carried out for the Rustenburg Layered Suite in the eastern Bushveld Complex. The Rustenburg Layered Suite consists of the Marginal Zone, Lower Zone, Critical Zone, Main Zone and Upper Zone. The mineral texture and chemical compositional variations were examined from the Lower to the Upper Zone. Although the number of sample is small, the crystallization sequence and presence of two types of magma can be recognized from the following mineral textures and compositions:

(1) Plagioclase occurs as a post-cumulus phase in rocks from the Lower Zone to lower subzone in the Critical Zone, whereas it occurs as a cumulus phase in rocks from the upper subzone in the Critical Zone, Main Zone and Upper Zone.

(2) A distinctive compositional difference of plagioclase and orthopyroxene can be seen between the lower subzone and upper subzone in the Critical Zone. In the lower subzone in the Critical Zone, post-cumulus plagioclase has low An within the range of 74–50, whereas the upper subzone has An=83–63.

This result is consistent with previous work. In addition, Norite in the upper subzone in the Critical Zone has orthopyroxene-developed (Opx-rich) and clinopyroxene-developed (Cpx-rich) domains. In the Opx-rich domain, high- X_{Mg} orthopyroxene and low-An plagioclase inclusions can be seen. On the other hand, both low- X_{Mg} orthopyroxene inclusions and high-An plagioclase inclusions are observed in the Cpx-rich domain. These textural and compositional relationships suggest possible magma mixing on the thin section scale.

key words: Rustenburg Layered Suite, Bushveld Complex, mineral texture, mineral chemistry, magma mixing

1. Introduction

Studies of layered igneous intrusions can provide important constrains to crystallization and chemical evolution in crustal magma chambers (Wilson, 1989). Typical examples of layered igneous intrusions are the Skaergaard intrusion in Greenland, the Stillwater Complex in Montana, and the Bushveld Complex in South

Africa. Of these, the Bushveld Complex is the largest layered intrusion in the world, covering an area of approximately 66000 km², and makes an 8-km-thick sequence of layered igneous rocks (Wager and Brown, 1968). The complex intrudes the Transvaal succession (~2.2 Ga: Tankard *et al.*, 1982), during 2.05–1.65 Ga. In addition, the mafic rocks of the Bushveld Complex are a major repository of PGE minerals, such as chromite and vanadiferous magnetite. On the basis of reversals of the normal fractionation trend, Cameron (1980) proposed that changing total pressure influences evolution. Further petrological studies (*e.g.* Mitchell, 1990) and Sr initial ratio profile (*e.g.* Kruger, 1992) indicate that two main magma types were involved in its evolution, and is now widely accepted (see Von Gruenewaldt *et al.*, 1985; Eales *et al.*, 1993). However, it is not fully investigated whether the compositional difference of constituent minerals related to their occurrences observed in individual rock.

Field work was carried out during March 16–17, 2000, to study the layered igneous intrusion, covering areas from lower to upper successions throughout the layered complex. The purpose of this paper is to briefly introduce the geology and petrography of the Rustenburg Layered Suite in the Bushveld Complex. In this paper, we investigate the relationships of the crystallization sequence from a small number of samples. Mineral texture and chemical compositions suggest that two main types of magmas are present and they are mixing on a thin section scale. Mineral abbreviations are after Kretz (1983) except for olivine (Olv).

2. Geological background

The Bushveld Complex forms horse-shoe shaped belts of mafic rocks, surrounding an acid central part, and is divided into the Rustenburg Layered Suite (2.05 Ga), the Rhashoop Granophyre Suite (>2.05 Ga) and the Lebowa Granite Suite (2.0 to 1.65 Ga) (Fig. 1). They intruded into the Transvaal Supergroup, which is divided into four groups: the Wolkberg Group, the Chuniespoort Group (volcanic and immature sedimentary rock), the Pretoria Group (sedimentary and volcanic deposits) and the Rooiberg Group (basic to felsic rock) (Wallmach *et al.*, 1995). The Rooiberg Group is overlain by an acidic volcanic succession (Loscop Formation). The Loscop Formation has a similar age to the Rooiberg Group (2.05 Ga).

The Rustenburg Layered Suite is subdivided into five major zones, namely the Marginal Zone, Lower Zone, Critical Zone, Main Zone and Upper Zone (Hall, 1932), and they vary more Fe-rich and felsic compositions towards upper unit (dunite and orthopyroxenite dominated in the lower unit, and norite-anorthosite, gabbro and diorite are dominated in the upper unit). The detailed stratigraphic units determined by the South Africa Council are given in Fig. 2.

The Rhashoop Granophyre Suite is composed of acidic granophyre, microgranophyre, and porphyritic granophyre rocks. Several hypotheses have been proposed for the origin of the Granophyre Suite (Tankard *et al.*, 1982 and references therein). At the contact of the Rustenburg Layered Suite with the overlying Transvaal Supergroup (felsites: Rooiberg Group), granophyres are considered as partial/complete melt from felsites. In other places, direct crystallization from magma is genetically related to the later Lebowa Granite Suite; metamorphism and partial melting of metasediment etc. have been

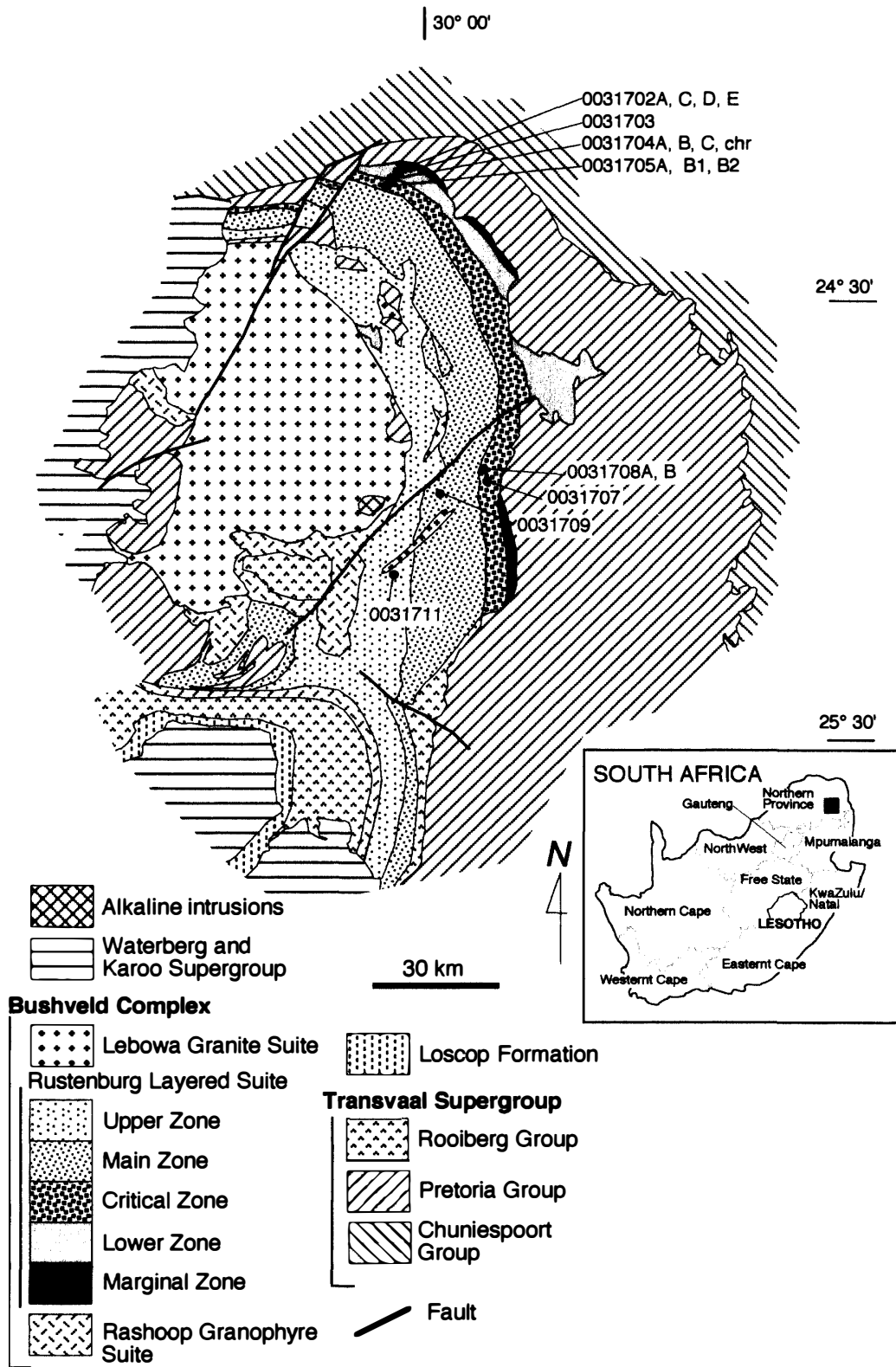


Fig. 1. Generalized geological map of the eastern part of the Bushveld Complex (Wallmach et al., 1995), showing sample localities.

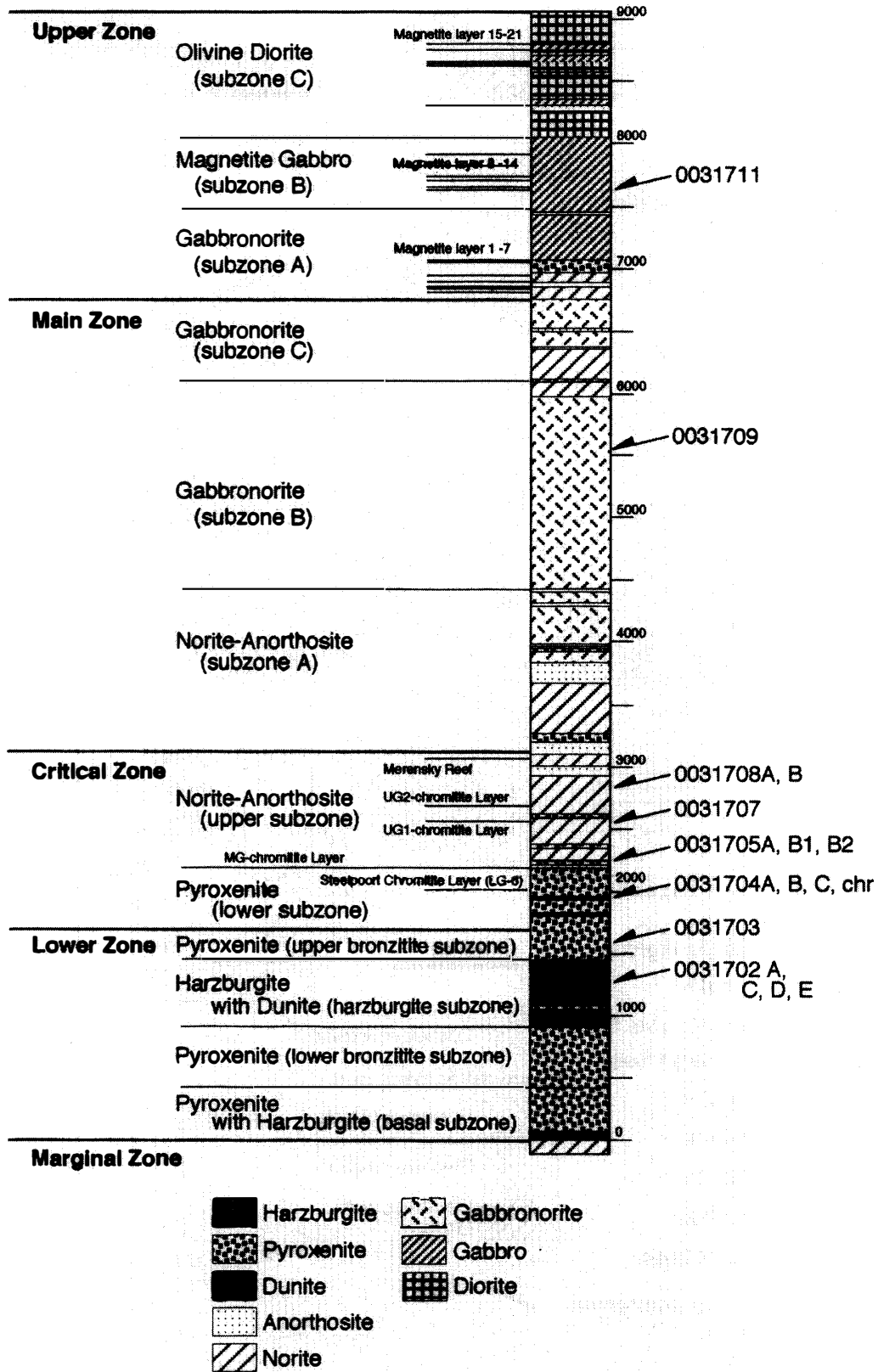


Fig. 2. Lithostratigraphic column of the Rustenburg Layered Suite in the eastern Bushveld Complex (Von Gruenewaldt *et al.*, 1985).

proposed, although there is no accepted view (Tankard *et al.*, 1982).

The Lebowa Granite Suite (Bushveld granite) represents the final phase of magmatic activity in the Bushveld Complex. It forms a large, sheet-like intrusion of batholithic dimensions generally intervening between the mafic rocks of the Rustenburg Layered Suite and the felsic rocks of the Rashedoep Granophyre Suite and Rooiberg Group. Two types of granite are identified, termed Nebo granite (showing variation from coarse grained gray granite, grading up through medium-grained gray and red granite) and Mukhutso granite (biotite-rich granite forming small dikes, sheets, and stocks). The Lebowa Granite Suite has typical features of A-type granites and represents the largest single body of A-type granites.

The Alkaline Intrusion can be seen at the western part of the Lebowa Granite Suite. It is composed of sequential intrusions of mica pyroxenite, ijolite and nepheline syenites with an eccentrically positioned, plug-like composite intrusion of carbonatite (Harmer and Gittins, 1997). The intrusion age has been dated at ~1.34 Ga (Harmer and Gittins, 1997). The Waterberg and Karro Supergroups are post-Bushveld cover sediments.

3. Lithological variation of the Rustenburg Layered Suite

3.1. Marginal Zone

The lowest part of the intrusion, namely the Marginal Zone (approximately 100 m thick), consists of fine-grained plagioclase-orthopyroxene cumulate, and contains abundant xenoliths. This zone, considered to be formed by relatively rapid cooling of the original undifferentiated magma, therefore, is representative of the parental magma (Davies *et al.*, 1980). Harmer and Sharpe (1985) have shown a strong chemical and isotopic relation between rocks of the Marginal Zone and the layered suite.

3.2. Lower Zone

Above the Marginal Zone is a Lower Zone (1700 m-thick), which consists of alternating layers of orthopyroxenite, dunite and harzburgite in the eastern limb (Cameron, 1978), and is subdivided into four subzones, basal subzone, lower bronzitite (pyroxenite) subzone, harzburgite subzone, and upper pyroxenite subzone (Cameron, 1978). The basal subzone consists mainly of feldspathic pyroxenite with minor harzburgite and norite layers. Upper and lower pyroxenite subzones are nearly monomineralic rocks containing orthopyroxene and minor amounts of plagioclase and clinopyroxene. The harzburgite subzone intervening between the upper and lower pyroxenite subzones consists of an alternating assemblage of harzburgite and pyroxenite (Cameron, 1978). The modal proportions and textures of olivine and orthopyroxene vary, and the rock type grades into olivine-pyroxenite and pyroxenite. Toward the top of the Lower Zone numerous thin layers of chromitite occur.

3.3. Critical Zone

This zone has been subdivided into two zones, a lower subzone (Zwartkoppies pyroxenite) and an upper subzone (Winterveld norite-anorthosite), on the basis of the appearance of cumulus plagioclase (*e.g.* Cameron, 1980). The former is mainly composed of pyroxenite with interlayered harzburgite and dunite, and the latter of norite and

anorthosite. Many chromitite layers, termed the LG- and UG-series, occur throughout this zone. Steelpoort Chromitite Layer (LG-6), 300 m above the base of this zone, is one of the most prominent stratigraphic marker. The top of the Critical Zone is marked by the Merensky Reef, the world's most important source of platinum (Von Gruenewaldt *et al.*, 1985).

3.4. Main Zone

Above the Merensky Reef is the Main Zone, consisting of 3600 m of poorly layered gabbroic rocks. It lacks the fine scale layering observed in the Critical Zone. This zone has been subdivided into three subzones, subzone A (mottled anorthosite and porphyritic norite), subzone B (homogeneous gabbronorites), and subzone C (norite-anorthosite and gabbronorite). Boundaries of these subzones are marked by the composition of the mineral which occurs as cumulus phase (Von Gruenewaldt, 1973). As a whole, the minerals in this zone show a steady upward variation to more fractionated compositions.

3.5. Upper Zone

The appearance of magnetite as a cumulus phase marks the beginning of the Upper Zone, which consists of 1500 m of ferrodiorites. Numerous magnetite cumulate layers occur near the base of this zone. Among these, the main magnetite layer forms a prominent stratigraphic marker that can be traced throughout the eastern and western limbs of the Rustenburg Layered Suite.

4. Sample description

4.1 Lower Zone

Rock samples from the Lower Zone were collected along the exposure at Olifants River trough, called the "Cameron Section", from the lower sequence to the upper sequence in the harzburgite subzone.

Harzburgite (0031702A): The rock was collected near the base of the harzburgite subzone. The rock consists of olivine, orthopyroxene and chromite, and is layered with dunite, individual layers ranging from centimeters to tens of meters in thickness, and contains pods composed of large grains of orthopyroxene. Olivine occurs as cumulus phase; the marginal parts are replaced by serpentine and calcite. Poikilitic orthopyroxene grains, up to 20 mm across, enclose rounded olivine grains and chromite (Fig. 3B). Chromite can be seen throughout the thin section.

Dunite (0031702C, 0031702D): This rock type, exposed interlayered within the harzburgite, is composed predominantly of cumulus olivine with minor chromite (Fig. 3A). The secondary minerals serpentine, calcite and tremolite replace olivine crystals. They developed along the crack.

Harzburgite (0031702E)-Olivine-orthopyroxenite (0031703): Toward the top of the sequence, both olivine and orthopyroxene occur as cumulus minerals. Both rocks have similar assemblages and textures, but the modal proportion of olivine and orthopyroxene changes. These rocks consist of orthopyroxene, olivine, clinopyroxene and chromite. Plagioclase and phlogopite occur as traces (Figs. 3C and 3D). Orthopyroxene crystals are euhedral to subhedral and display lamellae structure parallel to the (100) plane (Bushveld

type). Some olivine grains are subhedral to anhedral (postcumulus shape) relative to orthopyroxene grains (Fig. 4A). In places, a minor amount of clinopyroxene is seen. Chromite occurs both as inclusions and grain boundaries of other constituent minerals. Small amounts of plagioclase (0031702E) and phlogopite can be seen at the margins of orthopyroxene and clinopyroxene.

4.2. Critical Zone

4.2.1 Lower subzone of Critical Zone

Rock samples were collected from the lower to the upper sequence in this zone. Chromitites and orthopyroxenites were collected from the lower to the upper sequence (0031704A → 0031704chr → 0031704B → 0031704C) at an old quarry.

Chromitite (0031704chr) : The rock was collected from the Steelpoort Chromitite Layer (LG-6) which is about 1 m thick and can be traced continuously along the strike. It consists of chromite, plagioclase and orthopyroxene. Fine grained chromite (0.2–0.3 mm) with euhedral shapes is observed throughout a thin section (Fig. 3E). Poikilitic plagioclase and orthopyroxene develop enclosing a fine grained chromite. Orthopyroxene grains reach up to 3 mm in diameter.

Orthopyroxenites (0031704A, 0031704B and 0031704C): These rocks are observed in the lower and upper sequences of the chromitite layer (LG-6; Fig. 2). They are composed of orthopyroxene, plagioclase, chromite (Fig. 3F) and minor clinopyroxene. Orthopyroxene occurs as cumulus grain with Bushveld type exsolution lamellae. Chromite is generally observed at the margins of orthopyroxene, and occasionally as fine inclusions within orthopyroxene. Plagioclase is a post-cumulus mineral. Most of the clinopyroxene occurs as a late-stage mineral enclosing cumulus orthopyroxene grains. Tiny irregular shaped clinopyroxene sometimes occurs within orthopyroxene, presumably exsolved as lamellae. Minor phlogopite can be seen around the margin of orthopyroxene and chromite grains.

4.2.2 Upper subzone of Critical Zone

Anorthosite (0031705A)–Norite (0031705B1, 0031705B2): These rocks belong to the Winterveld norite-anorthosite. Both rocks were sampled from large boulders located near the base of this subzone. Anorthosite (0031705A) consists of plagioclase, orthopyroxene, and a small amount of clinopyroxene (Fig. 3G). Cumulus plagioclase, up to 3 mm in length, is predominant. Cumulus orthopyroxene contains tiny inclusions of plagioclase, and is occasionally rimmed by clinopyroxene. Clinopyroxene occurs as interstitial grains. A minor amount of chromite can be seen, but in less amount compared to those exposed in the lower subzone. The texture of the sample 0031705B1 is similar to that of 0031705A, although the former sample is slightly rich in clinopyroxene. Clinopyroxene often contains tiny plagioclase grains. In addition, the clinopyroxene occasionally shows exsolution lamellae roughly parallel to (001) and (100) (Fig. 4B). In places, a poikilitic clinopyroxene grain encloses rounded orthopyroxene. The rock contains no chromite.

Norite (0031705B2): This rock shows a distinctive texture, that is, there are post-cumulus (poikilitic) orthopyroxene-developed (Opx-rich) and fine clinopyroxene-developed (Cpx-rich) domains (Figs. 3H and 4C). The cumulus plagioclase texture is similar to that of anorthosite, and can be seen in both domains. Poikilitic orthopyroxene grains, up to 8 mm in diameter, are well developed, and enclose cumulus plagioclase and tiny rounded plagioclase grains. Fine clinopyroxene grains (0.2–0.3 mm) sometimes include tiny

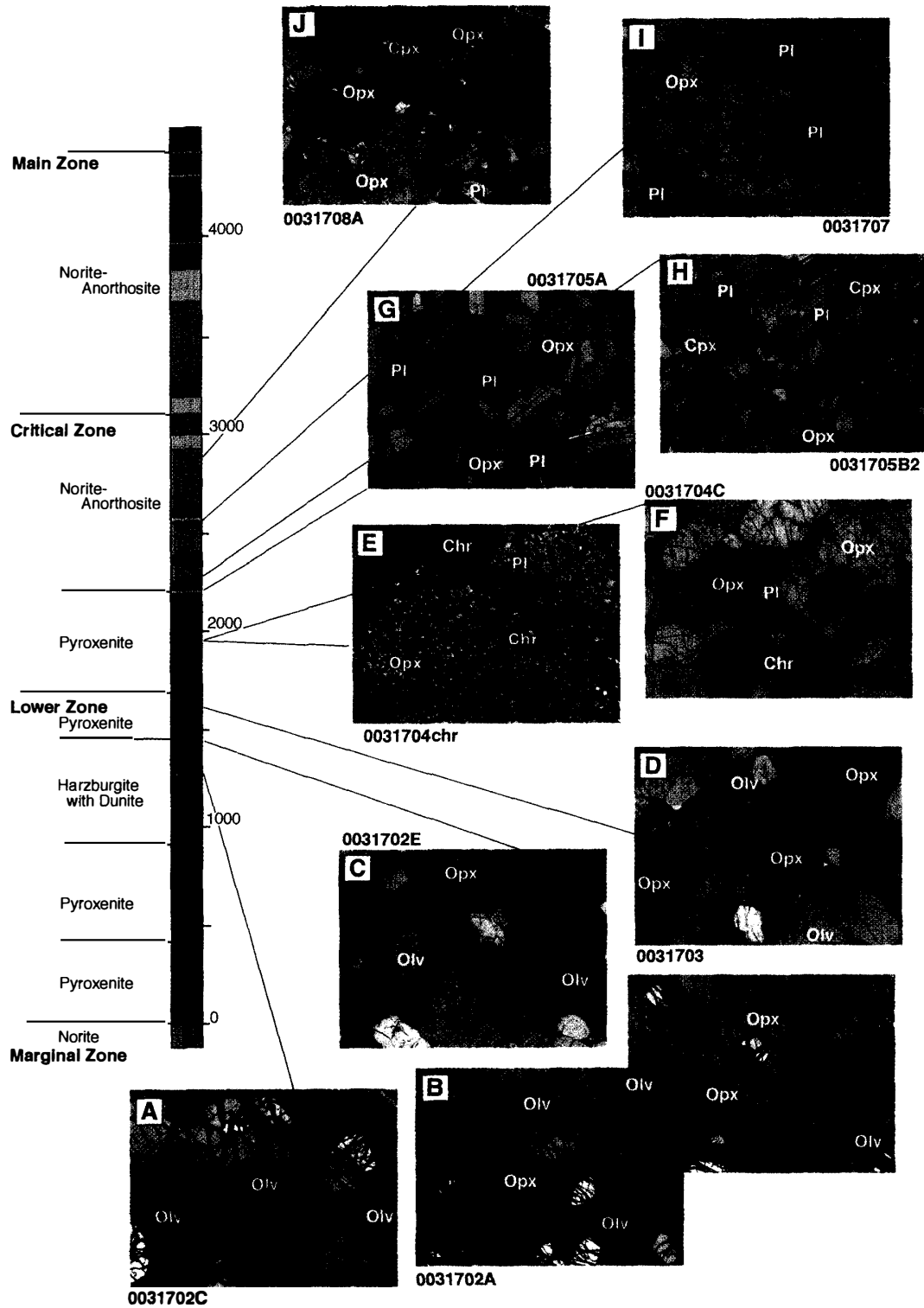


Fig. 3. Photomicrographs of the constituent minerals showing the lithostratigraphic column. A, Dunite (0031702C); B, Harzburgite (0031702A); C, Harzburgite (0031702E); D, Olivine-orthopyroxenite (0031703); E, Chromitite (0031704chr); F, Orthopyroxenite (0031704); G, Anorthosite (0031705A); H, Norite (0031705B2); I, Anorthosite (0031707); J, Norite (0031708A); K, L & M, Gabbro (0031709); N, O & P, Gabbro (0031711). The width of each photomicrograph is 4.6 mm, excluding M and P (3 mm).

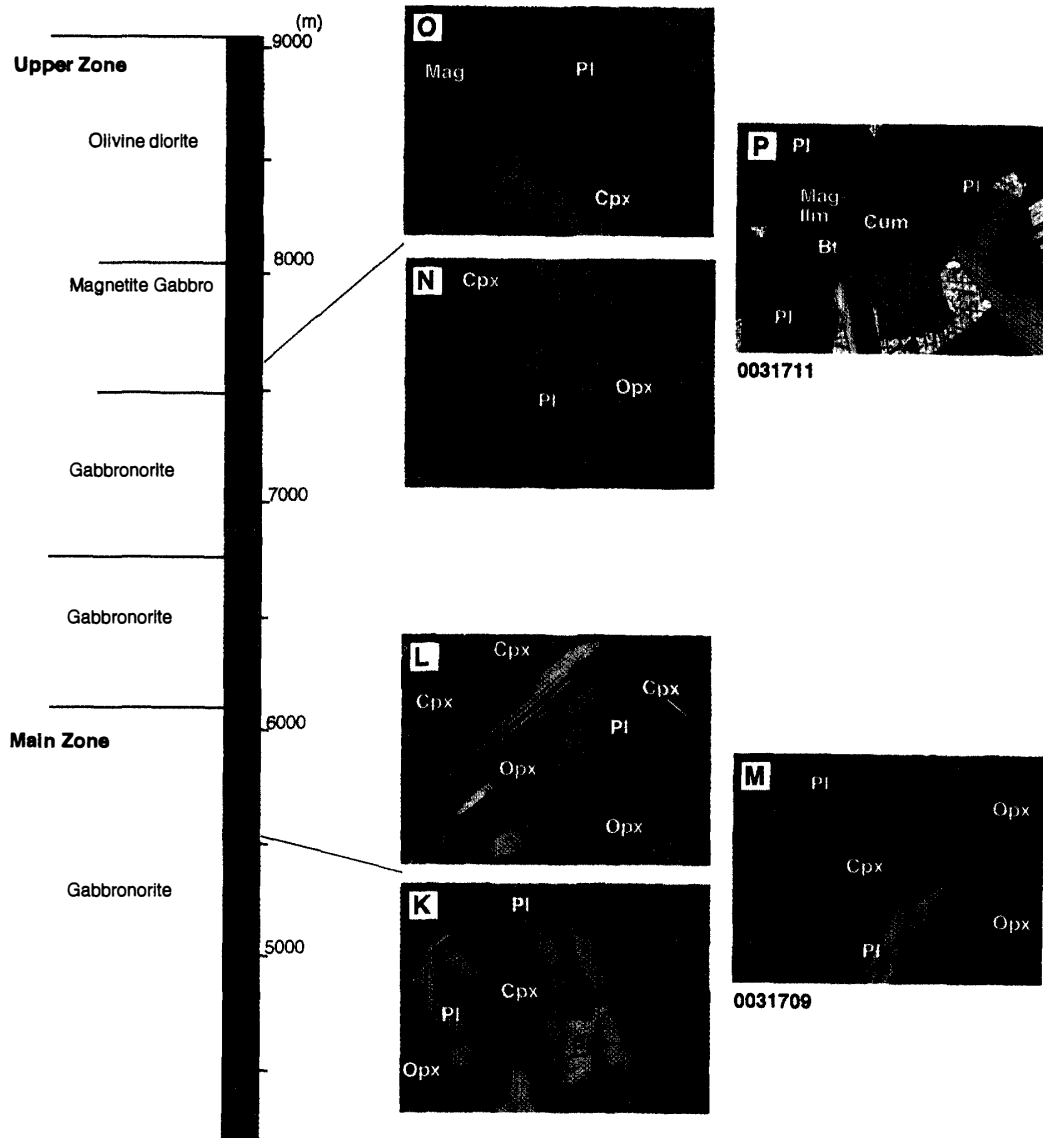


Fig. 3 (continued).

rounded orthopyroxene (apart from linear shaped exsolution lamellae) and plagioclase grains.

Anorthosite (0031707): The anorthosite boulder was collected near the National Monument near the Dwars River. In this locality, the chromitite layer (UG-1; Fig. 2) and its footwall anorthosite are well exposed, and display complicated relationships. In places, several deformation structures due to magmatic flow can be seen. The rock consists predominantly of cumulus-plagioclase, orthopyroxene, chromite and trace clinopyroxene (Fig. 3I). Orthopyroxene appears as a post-cumulus mineral enclosing euhedral to subhedral plagioclase. Minor clinopyroxene also occurs as a later phase, and is sometime observed along the margins of orthopyroxene. Thin layers, consisting of aligned chromite grains, can be seen in the thin section. Fine chromite grains also occur

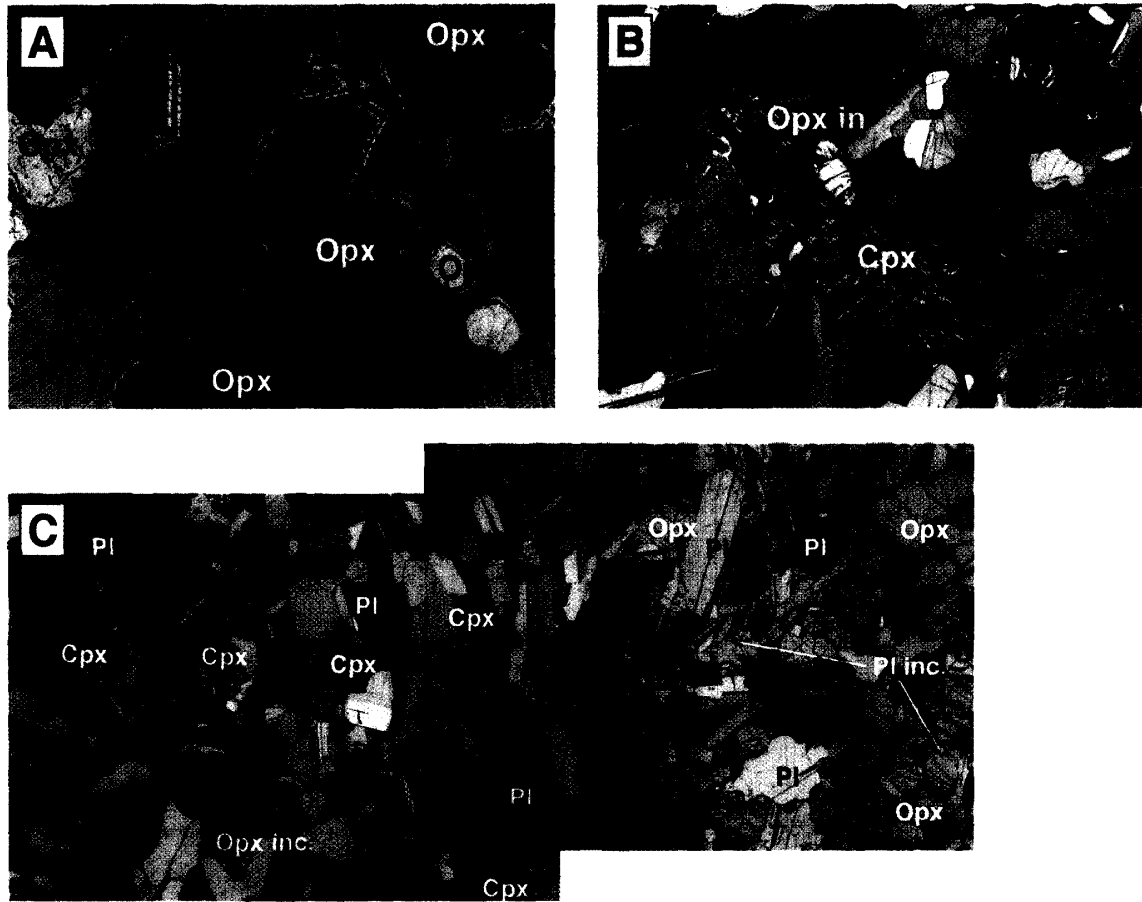


Fig. 4. Photomicrographs showing characteristic mineral textures. A, Olivine occurs as post-cumulus grain with including rounded orthopyroxene. Triangular scrap of orthopyroxene is separated from original cumulus orthopyroxene by olivine (0031702E). The width of photomicrograph is 3 mm. B, Rounded orthopyroxene inclusion (Opx in) and two directions of exsolution lamellae can be seen in the clinopyroxene (0031705B1). The width of each photomicrograph is 4 mm. C, Poikilitic orthopyroxene developed-domain (right part) and fine-grained clinopyroxene developed-domain (left part) can be seen in a single thin section (0031705B2). Cumulus plagioclases occur throughout the thin section, and are enclosed by poikilitic orthopyroxene. Tiny rounded plagioclase (Pl inc) can be seen as inclusion within poikilitic orthopyroxene. Fine clinopyroxene includes tiny rounded plagioclase and orthopyroxene (Opx inc). The width of each photomicrograph is 7.5 mm.

as tiny inclusions within the orthopyroxene. A small amount of secondary biotite can be seen at the margin of the orthopyroxene.

Norite (0031708A, 0031708B): Orthopyroxene and plagioclase appear as cumulus minerals. Orthopyroxenes contain numerous inclusions of fine plagioclase and clinopyroxene grains, and are often rimmed by clinopyroxene (Fig. 3J). Some linear clinopyroxene inclusions parallel to the Bushveld type exsolution lamellae might be in the exsolved phase. Clinopyroxene also occurs as a post-cumulus phase, which includes rounded orthopyroxene and plagioclase.

4.3. Main Zone

Rock samples were collected from the roadside isolated outcrop. They are coarse-grained and show a preferred orientation defined by plagioclase and clinopyroxene in hand specimens, possibly formed by magmatic flow.

Gabbro (0031709): The rock is composed of plagioclase, clinopyroxene, and orthopyroxene, with accessory hornblende, biotite and magnetite (Figs. 3K and 3L). Ophitic texture with large euhedral grains of plagioclase with anhedral clinopyroxene and poikilitic orthopyroxene can be seen. Clinopyroxene commonly has exsolution lamellae of orthopyroxene (Fig. 3M), showing two orientations roughly parallel to (100) and (001). Apart from these exsolution lamellae, clinopyroxene contains rounded orthopyroxene grains. The orthopyroxene dominant part shows poikilophitic texture with enclosed euhedral plagioclase. Hornblende and biotite occur as secondary minerals around the margins of pyroxenes. Accessory minerals occur as inclusions within clinopyroxene, and in the matrix.

4.4. Upper Zone

Gabbro (0031711): The ophitic texture, plagioclase joined as euhedral/subhedral mosaic with small amount of clinopyroxene confined to the corner of the plagioclase, can be seen. The modal proportion of plagioclase is higher than that in gabbro in the Main Zone (0031709). Plagioclase, clinopyroxene and magnetite-ilmenite are main constituent mineral (Figs. 3N and 3O), and biotite and symplectic Fe-rich cummingtonite ($Mg/(Mg+Fe)=0.35-0.40$) occur as traces. Plagioclase, up to 2.5 mm in length, has tiny needles of rutile. Clinopyroxene commonly has exsolution lamellae of orthopyroxene, and they often show two orientations parallel to (100) and (001). Magnetite-ilmenite are rimmed by biotite, which in turn is surrounded by symplectic cummingtonite and plagioclase (Fig. 3P).

5. Chemistry of the constituent minerals

Chemical analyses of constituent minerals were performed using an electron microprobe with a wavelength-dispersive X-ray analytical system (JEOL JXA-8800M) at the National Institute of Polar Research. All mineral analyses were performed under accelerating voltage of 15 kV and specimen current of 12 nA. Natural minerals and synthetic oxides were used as standards. Mineral compositional data are presented in Tables 1, 2, and 3.

5.1. Plagioclase

Figure 5 shows the composition of plagioclase in rocks from the Lower Zone (LZ) to the Upper Zone (UZ). In the lower subzone of the Critical Zone (LCZ), plagioclase appears as post-cumulus phase (e.g. Fig. 3E & F), and has An content of 74–50. The lowest anorthosite layer (0031705A) in the base of the upper subzone of the Critical Zone (UCZ), records maximum An content of 83–80, and then An content gradually decreases upward. The distinctive compositional difference reflects the shape of plagioclase; for instance, the cumulus phase in the upper sequence has high An, while the post-cumulus phase has low An content. Post-cumulus plagioclase in harzburgite

Table 1. Representative microprobe analyses of constituent minerals.

Sample No. Anal. No. Mineral	Lower Zone						Critical Zone (lower subzone)							
	0031702A			0031702C		0031402E		0031703		0031704chr				
	1 Olv core	4 Opx poiki	9 Chr in Oliv	40 Olv core	45 Chr in Oliv	3 Opx core	6 Olv core	17 Opx core	82 Opx core	86 Olv core	88 Chr in Opx	34 Opx poiki	38 Chr core	43 Pl in Opx
SiO ₂	41.38	57.35	0.02	40.97	0.03	56.98	40.39	56.38	57.05	41.21	0.04	57.00	0.00	50.90
TiO ₂	0.05	0.00	0.50	0.01	0.53	0.15	0.01	0.05	0.06	0.01	0.43	0.11	1.24	0.00
Al ₂ O ₃	0.04	1.31	15.80	0.00	15.95	1.32	0.00	1.34	1.24	0.03	16.37	1.17	14.67	31.13
Cr ₂ O ₃	0.00	0.47	46.58	0.03	40.34	0.50	0.01	0.42	0.45	0.05	46.15	0.41	44.47	0.04
FeO*	11.86	7.70	26.38	12.31	33.84	7.99	12.48	7.48	7.86	12.41	26.33	9.66	30.35	0.16
MnO	0.15	0.15	0.34	0.19	0.40	0.15	0.16	0.13	0.17	0.15	0.32	0.17	0.22	0.03
MgO	47.10	32.67	9.16	46.73	6.01	32.26	46.82	30.68	32.44	47.59	8.75	31.15	6.79	0.02
CaO	0.06	0.94	0.00	0.00	0.02	0.75	0.00	3.42	0.88	0.06	0.02	0.48	0.04	14.13
Na ₂ O	0.02	0.00	0.00	0.01	0.06	0.06	0.01	0.11	0.03	0.04	0.01	0.03	0.07	3.36
K ₂ O	0.00	0.06	0.00	0.00	0.00	0.00	0.00	0.00	0.00	0.00	0.00	0.00	0.00	0.24
Total	100.65	100.63	98.73	100.25	97.18	100.16	99.88	100.01	100.18	101.55	98.42	100.18	97.85	100.01
O	4	6	4	4	4	6	4	6	6	4	4	6	4	8
Si	1.014	1.979	0.001	1.011	0.001	1.978	1.002	1.972	1.979	1.005	0.001	1.989	0.000	2.319
Ti	0.001	0.000	0.012	0.000	0.013	0.004	0.000	0.001	0.002	0.000	0.011	0.003	0.031	0.000
Al	0.001	0.053	0.608	0.000	0.635	0.054	0.000	0.055	0.051	0.001	0.632	0.048	0.581	1.671
Cr	0.000	0.013	1.202	0.001	1.077	0.014	0.000	0.012	0.012	0.001	1.196	0.011	1.182	0.001
Fe ³⁺	-	-	0.163	-	0.263	-	-	-	-	-	0.148	-	0.179	0.010
Fe ²⁺	0.243	0.222	0.558	0.254	0.692	0.232	0.259	0.219	0.228	0.253	0.573	0.282	0.674	-
Mn	0.003	0.004	0.009	0.004	0.011	0.004	0.003	0.004	0.005	0.003	0.009	0.005	0.006	0.001
Mg	1.720	1.680	0.446	1.719	0.303	1.669	1.732	1.599	1.677	1.729	0.428	1.620	0.340	0.001
Ca	0.001	0.035	0.000	0.000	0.001	0.028	0.000	0.128	0.033	0.002	0.001	0.018	0.001	0.690
Na	0.001	0.000	0.000	0.000	0.004	0.004	0.000	0.007	0.002	0.002	0.001	0.002	0.005	0.297
K	0.000	0.002	0.000	0.000	0.000	0.000	0.000	0.000	0.000	0.000	0.000	0.000	0.000	0.014
Total cation	2.985	3.989	3.000	2.989	3.000	3.986	2.998	3.997	3.989	2.995	3.000	3.979	3.000	5.004
X _{Mg}	0.88	0.88	0.44	0.87	0.30	0.88	0.87	0.88	0.88	0.87	0.43	0.85	0.34	-
Wo	-	0.02	-	-	-	0.01	-	0.07	0.02	-	-	0.01	-	-
X _{An}	-	-	-	-	-	-	-	-	-	-	-	-	-	0.70

FeO*, total Fe as FeO; Fe³⁺ is estimated from charge balance; poiki, as poikiloblast; inter, intersertal grain; in Oliv, inclusion within Oliv; Opx marg, marginal part of Opx.

Table 2. Representative microprobe analyses of constituent minerals.

Sample No. Anal. No. Mineral	Critical Zone (lower subzone)						Critical Zone (upper subzone)							
	0031704A			0031704B			0031705 B2			0031707				
	91 Opx core	99 Cpx Opx marg	118 Pl inter	147 Opx core	154 Cpx core	161 Pl inter	76 Opx poiki	92 Pl in Opx	88 Pl core	107 Opx in Cpx	110 Pl in Cpx	41 Pl core	53 Cpx Opx marg	71 Opx core
SiO ₂	56.93	54.26	52.18	57.34	53.87	51.59	54.81	52.84	50.83	55.10	49.68	49.63	53.61	54.41
TiO ₂	0.08	0.30	0.00	0.08	0.21	0.08	0.29	0.03	0.02	0.15	0.04	0.05	0.20	0.23
Al ₂ O ₃	1.23	1.73	31.39	1.18	2.15	31.41	0.88	28.75	31.73	0.91	32.40	31.61	1.08	1.10
Cr ₂ O ₃	0.48	0.68	0.06	0.43	1.05	0.00	0.21	0.00	0.00	0.31	0.00	0.00	0.53	0.35
FeO*	10.31	3.49	0.16	9.52	3.80	0.18	14.43	0.88	0.28	15.74	0.26	0.27	6.28	18.29
MnO	0.21	0.14	0.05	0.23	0.14	0.00	0.30	0.03	0.05	0.33	0.00	0.00	0.16	0.39
MgO	31.30	16.02	0.03	32.12	16.18	0.03	28.21	0.61	0.00	26.70	0.00	0.06	15.15	25.11
CaO	0.62	23.24	13.65	0.64	22.68	14.02	0.97	10.92	15.01	0.59	15.77	15.58	22.57	0.25
Na ₂ O	0.03	0.34	3.50	0.02	0.40	3.56	0.01	4.53	2.96	0.00	2.57	2.53	0.27	0.02
K ₂ O	0.00	0.00	0.22	0.00	0.00	0.20	0.00	0.13	0.16	0.00	0.14	0.18	0.00	0.00
Total	101.19	100.20	101.24	101.56	100.48	101.07	100.11	98.72	101.04	99.83	100.86	99.91	99.85	100.15
O	6	6	8	6	6	8	6	8	8	6	8	8	6	6
Si	1.976	1.973	2.341	1.976	1.957	2.323	1.963	2.424	2.296	1.988	2.253	2.271	1.980	1.980
Ti	0.002	0.008	0.000	0.002	0.006	0.003	0.008	0.001	0.001	0.004	0.001	0.002	0.006	0.006
Al	0.050	0.074	1.660	0.048	0.092	1.667	0.037	1.554	1.689	0.039	1.732	1.705	0.047	0.047
Cr	0.013	0.020	0.002	0.012	0.030	0.000	0.006	0.000	0.000	0.009	0.000	0.000	0.015	0.010
Fe ³⁺	-	-	0.006	-	-	0.007	0.015	0.034	0.011	-	0.010	0.010	-	-
Fe ²⁺	0.299	0.106	-	0.274	0.115	-	0.417	-	-	0.475	-	-	0.194	0.557
Mn	0.006	0.004	0.002	0.007	0.004	0.000	0.009	0.001	0.002	0.010	0.000	0.000	0.005	0.012
Mg	1.619	0.868	0.002	1.649	0.876	0.002	1.506	0.042	0.000	1.436	0.000	0.004	0.834	1.362
Ca	0.023	0.906	0.656	0.024	0.883	0.677	0.037	0.537	0.726	0.023	0.766	0.764	0.893	0.010
Na	0.002	0.024	0.304	0.001	0.028	0.311	0.001	0.403	0.259	0.000	0.226	0.225	0.019	0.001
K	0.000	0.000	0.013	0.000	0.000	0.011	0.000	0.008	0.009	0.000	0.008	0.011	0.000	0.000
Total cation	3.991	3.984	4.986	3.993	3.991	5.002	4.000	5.003	4.994	3.984	4.997	4.991	3.993	3.986
XMg	0.84	0.89	-	0.86	0.88	-	0.78	-	-	0.75	-	-	0.81	0.71
Wo	0.01	0.48	-	0.01	0.47	-	0.02	-	-	0.01	-	-	0.46	0.01
XAn	-	-	0.68	-	-	0.69	-	0.57	0.74	-	0.77	0.77	-	-

Note on the eastern Bushveld Complex

Table 3. Representative microprobe analyses of constituent minerals.

Sample No. Anal. No. Mineral	Critical Zone (upper subzone) 0031708A				Main Zone 0031709					Upper Zone 0031711				
	157 Pl core	161 Pl rim	164 Opx core	184 Cpx Opx marg	182 Pl core	191 Pl mantle	193 Pl rim	201 Cpx inter	164 Opx lamalae	22 Pl core	23 Pl mantle	26 Pl rim	28 Opx lamalae	29 Cpx inter
SiO ₂	50.62	51.39	55.80	52.80	53.27	53.45	52.76	52.68	53.30	55.31	54.74	54.62	51.70	52.09
TiO ₂	0.03	0.02	0.13	0.46	0.08	0.07	0.00	0.35	0.15	0.04	0.06	0.02	0.21	0.40
Al ₂ O ₃	31.57	31.60	0.73	1.48	29.52	30.10	30.10	1.07	0.93	28.11	28.64	28.43	0.56	1.17
Cr ₂ O ₃	0.03	0.00	0.15	0.67	0.01	0.00	0.00	0.02	0.01	0.00	0.00	0.01	0.00	0.02
FeO*	0.29	0.23	15.20	5.59	0.32	0.35	0.34	8.91	22.83	0.27	0.10	0.16	28.74	11.55
MnO	0.00	0.00	0.31	0.11	0.08	0.05	0.00	0.29	0.46	0.01	0.00	0.04	0.66	0.30
MgO	0.04	0.03	28.32	15.26	0.02	0.02	0.01	13.62	22.09	0.01	0.01	0.03	17.20	12.52
CaO	14.84	13.94	0.43	22.88	12.35	12.46	13.10	21.72	0.68	10.90	11.14	11.58	1.06	22.01
Na ₂ O	2.96	3.14	0.02	0.31	4.21	4.23	4.06	0.36	0.02	5.25	4.99	4.79	0.02	0.16
K ₂ O	0.18	0.24	0.00	0.00	0.27	0.27	0.27	0.00	0.00	0.24	0.25	0.15	0.00	0.00
ZnO	0.00	0.00	0.00	0.00	0.00	0.00	0.00	0.00	0.00	0.00	0.00	0.00	0.00	0.00
Total	100.56	100.59	101.09	99.56	100.13	101.00	100.64	99.02	100.47	100.14	99.93	99.83	100.15	100.22
O	8	8	6	6	8	8	8	6	6	8	8	8	6	6
Si	2.297	2.322	1.982	1.955	2.412	2.399	2.382	1.983	1.979	2.492	2.471	2.470	1.987	1.961
Ti	0.001	0.001	0.003	0.013	0.003	0.002	0.000	0.010	0.004	0.001	0.002	0.001	0.006	0.011
Al	1.688	1.683	0.031	0.065	1.575	1.593	1.602	0.047	0.041	1.493	1.524	1.515	0.025	0.052
Cr	0.001	0.000	0.004	0.020	0.000	0.000	0.000	0.001	0.000	0.000	0.000	0.000	0.000	0.001
Fe ³⁺	0.011	0.009	-	0.003	0.012	0.013	0.013	-	-	0.010	0.004	0.006	-	0.015
Fe ²⁺	-	-	0.452	0.170	-	-	-	0.280	0.709	-	-	-	0.924	0.349
Mn	0.000	0.000	0.009	0.003	0.003	0.002	0.000	0.009	0.014	0.000	0.000	0.002	0.021	0.010
Mg	0.003	0.002	1.499	0.842	0.001	0.001	0.001	0.764	1.222	0.001	0.001	0.002	0.985	0.703
Ca	0.721	0.675	0.016	0.907	0.599	0.599	0.634	0.876	0.027	0.526	0.539	0.561	0.044	0.888
Na	0.260	0.275	0.001	0.022	0.370	0.368	0.355	0.026	0.001	0.459	0.437	0.420	0.001	0.012
K	0.010	0.014	0.000	0.000	0.016	0.015	0.016	0.000	0.000	0.014	0.014	0.009	0.000	0.000
Total cation	4.993	4.981	3.998	4.000	4.990	4.994	5.003	3.997	3.997	4.996	4.991	4.986	3.995	4.000
XMg	-	-	0.77	0.83	-	-	-	0.73	0.63	-	-	-	0.52	0.67
Wo	-	-	0.01	0.47	-	-	-	0.46	0.01	-	-	-	0.02	0.46
XAn	0.73	0.71	-	-	0.62	0.62	0.64	-	-	0.53	0.55	0.57	-	-

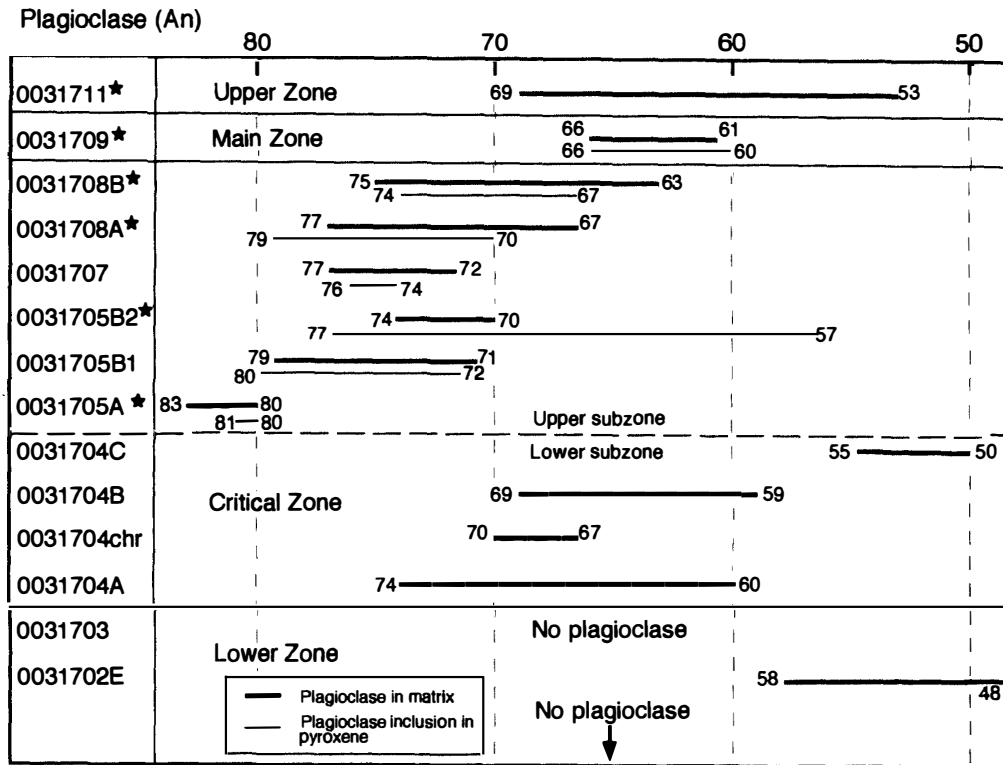


Fig. 5. Compositional variation of plagioclase. Thick lines and thin lines represent plagioclase in the matrix and inclusions within pyroxenes respectively. The samples labeledly stars are also plotted in Fig. 6.

(0031702E) from the LZ has low An content.

Some cumulus plagioclase optically shows zonal texture, although their compositional zonation is variable. Figure 6 shows a compositional plot of plagioclase grains from the UCZ to the Upper Zone (UZ). The compositional variation of each grain and the relation of the inclusion grain to the host mineral can be recognized in this figure. As shown in Fig. 6, plagioclase in 0031708A and 0031709 have fairly uniform composition. Inclusions within pyroxenes also have similar values. A normal zoning pattern, rimward decrease in An, can be seen in plagioclase from norite in the CZ (0031708B). On the other hand, rocks belonging to the Main Zone (MZ) and Upper Zone (UZ) (0031709 and 0031711), record maximum An content at the rims of plagioclase grains. Another distinctive variation can be seen in norite (0031705B2) from the UCZ. The tiny rounded plagioclase grains within orthopyroxene have the lowest An content (with $Fe_2O_3=0.88$ wt% and $MgO=0.61$ wt%; Table 2), whereas the grain within clinopyroxene records the highest An content (with $Fe_2O_3 =0.23-0.34$ wt% and $MgO=0.00-0.01$ wt%). This compositional difference between inclusion and matrix can be seen only in this rock. The TiO_2 content of plagioclase is considered to reflect magma composition (Togashi *et al.*, 1998), but is not discussed here due to analytical uncertain.

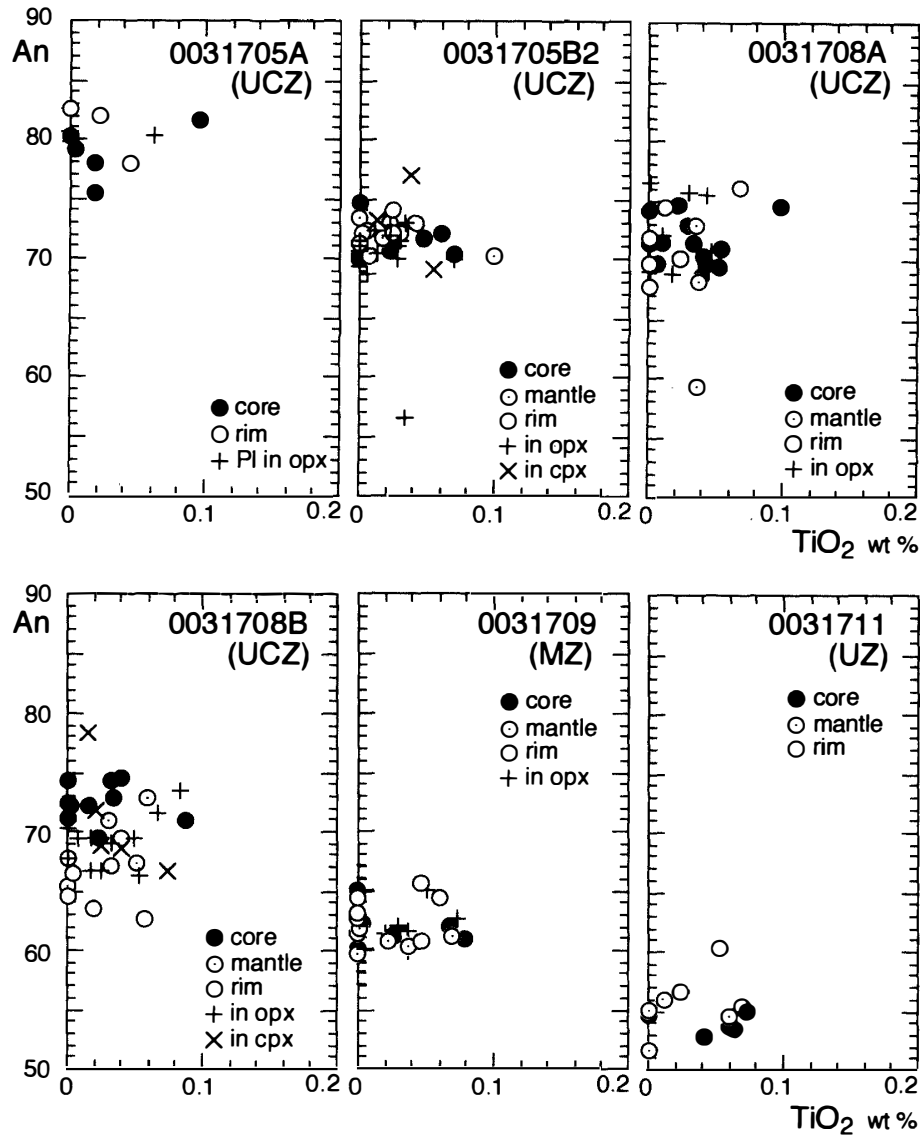


Fig. 6. An versus TiO_2 wt% compositional plot for selected plagioclase grains. Plagioclase TiO_2 wt% reflects magma composition (Togashi *et al.*, 1998), but is not given in the text due to analytical uncertainty. Core, central part of plagioclase grain; rim, marginal part of plagioclase grain; mantle, inner rim of plagioclase; pl in opx, plagioclase inclusion within orthopyroxene; pl in cpx, plagioclase inclusion within clinopyroxene.

5.2. Chromite

Chromite is a main constituent mineral in the LZ and LCZ. Irvine (1977) has shown experimentally that the $\text{Cr}/(\text{Cr}+\text{Al})$ ratios of chromite decrease with differentiation and falling temperature. Compositional features of chromite from the LZ and CZ are shown in Figs. 7A and B. As shown in Fig. 7B, chromite inclusions within the olivine have high $\text{Cr}/(\text{Cr}+\text{Al})$ ratios, whereas matrix chromite has low ratios in the same sample (0031702D). This compositional relationship implies that chromite crystallized earlier than olivine, and then olivine and matrix chromite are crystallized in the LZ. The wide

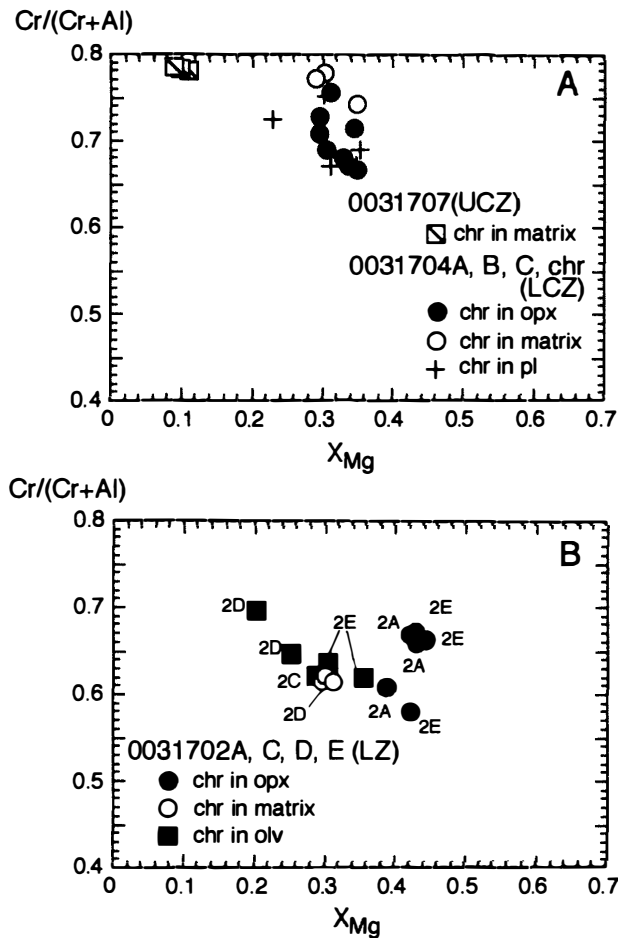


Fig. 7. Compositional variation of chromite in the Lower Zone (B) and Upper Zone (A). Chr in matrix, chromite occurs as grain boundary between constitute mineral; chr in opx/pl/olv, chromite grains occur as inclusions within orthopyroxene/plagioclase/olivine, respectively.

range of X_{Mg} ratios of chromite seems to reflect the whole rock compositions of each rock. On the other hand, in the CZ, matrix chromite (grain boundary) was crystallized earlier under high temperature, and then plagioclase and/or pyroxene were formed, enclosing low Cr/(Cr+Al) chromite.

5.3. Pyroxenes and olivine

Compositional variation of the pyroxenes and olivine is given in Fig. 8. A compositional difference regarding orthopyroxene X_{Mg} can be seen between LCZ and UCZ (Fig. 8); it probably reflects the difference in whole rock composition. In sample 0031705B2, orthopyroxene compositions in the Opx-rich and Cpx-rich domains are clearly distinguishable (Fig. 8). High X_{Mg} values of orthopyroxene are observed in the Opx-rich domain, low values in the Cpx-rich domain. The X_{Ca} ratio of clinopyroxene seems to decrease from LZ to the boundary of LCZ and UCZ. The trend is in harmony with the change of X_{Mg} ratios of the orthopyroxene. However, above the base of the UCZ, the compositional trend is variable. The X_{Mg} ratios of olivine do not show any notable decrease toward the upper sequence.

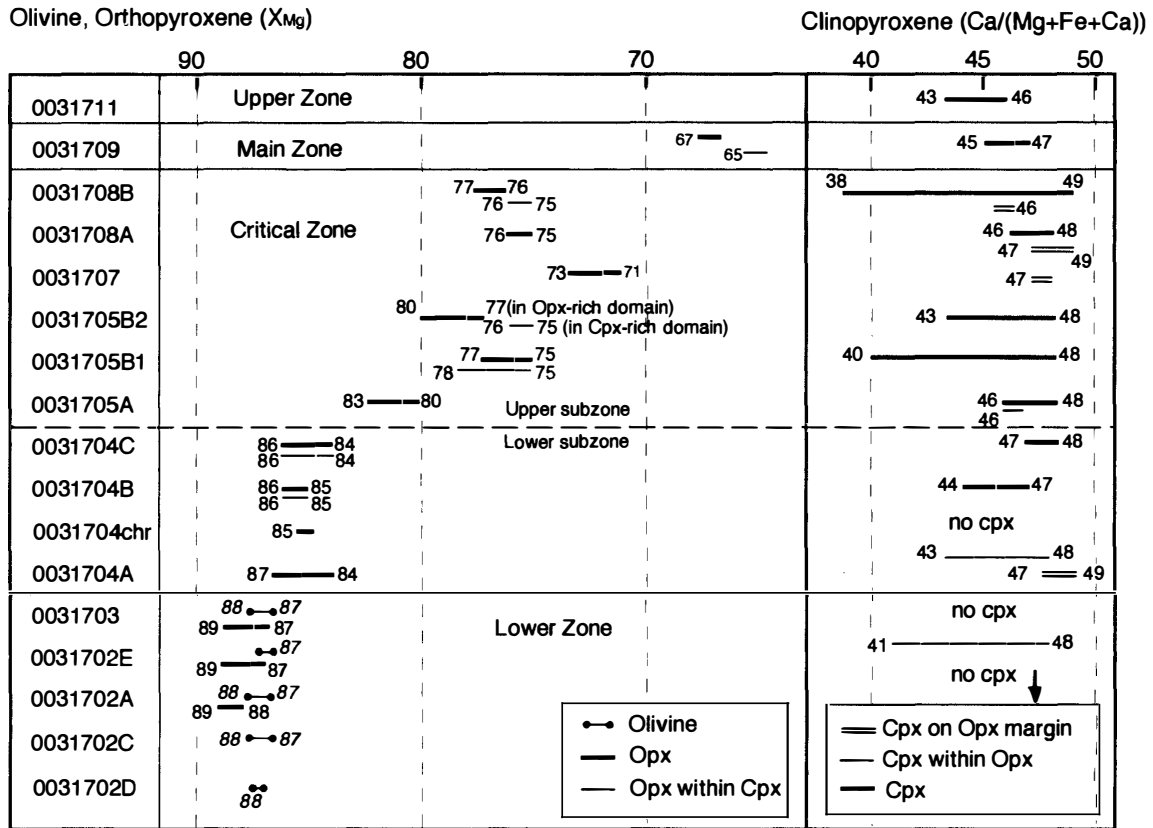


Fig. 8. Compositional variation of olivine, orthopyroxene and clinopyroxene. Opx within Cpx, orthopyroxene occurs as inclusions within clinopyroxene; Cpx on Opx margin, Clinopyroxene occurs marginal part of the orthopyroxene grains; Cpx within Opx, orthopyroxene inclusion within clinopyroxene.

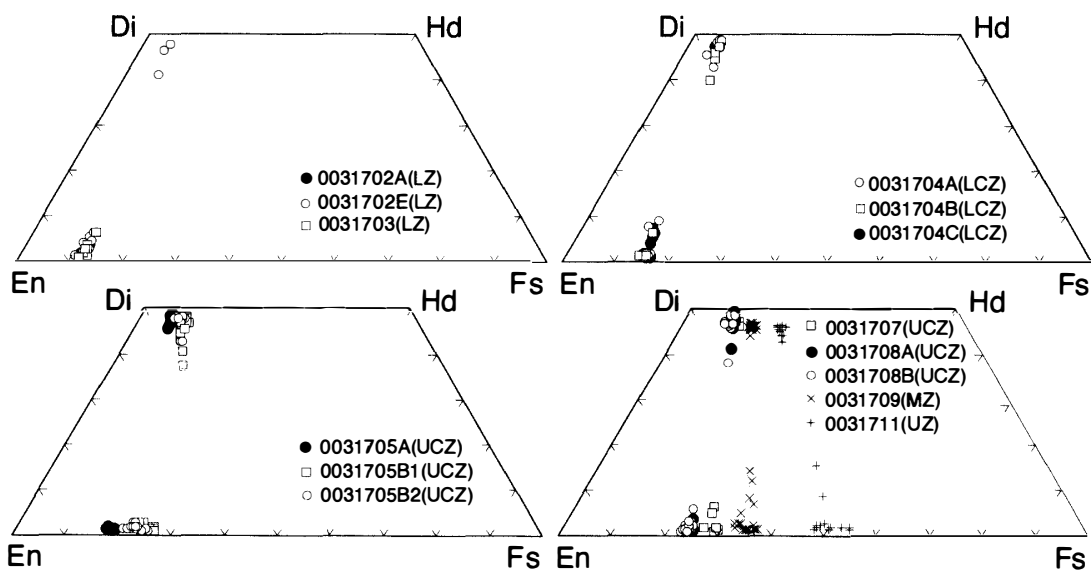


Fig. 9. Quadrilateral plot on En-Di-Hd-Fs for two pyroxene. The compositions in this figure. were drawn by using End-member regarding Fe^{2+} , Mg and Ca, and ignoring Na and Cr.

Orthopyroxene and clinopyroxene compositions are plotted in the pyroxene quadrilateral (Fig. 9). As a whole, orthopyroxene and clinopyroxene shifted to Fe-rich composition toward the upper sequences, and might represent fractional crystallization.

6. Discussion

6.1. Two types of magmas

Two types of magmas have been proposed by previous workers for the evolution of the Rustenburg Layered Suite (Davies *et al.*, 1980; Cawthorn *et al.*, 1981; Sharpe, 1981; Cawthorn and Davies, 1983; Sharpe and Irvine, 1983; Harmer and Sharpe, 1985). Sr-isotopic studies (Kruger, 1992; Cawthorn *et al.*, 1991; Lee and Butcher, 1990) also suggest the presence of two magma types.

The characteristics of mineral texture and composition in this study can be summarized as follows:

- (1) Plagioclase occurs as a post-cumulus phase in rocks from the LZ to LCZ, whereas it occurs as a cumulus phase in rocks from the UCZ, MZ and UZ.
- (2) Compositional difference of plagioclase and orthopyroxene can be seen between the LCZ and UCZ.
- (3) Chromite composition changed relative to its occurrences. In the LZ, high Cr/(Cr+Al) chromite is observed in cumulus olivine. On the other hand, in the CZ, high Cr/(Cr+Al) chromite occurs in the matrix together with plagioclase.

(1) and (2) probably support the presence of different types of crystallization sequence which are derived from two magmas. LZ-LCZ show a crystallization sequence of olivine → orthopyroxene → plagioclase. UCZ-MZ-UZ shows a sequence of plagioclase → orthopyroxene → clinopyroxene. Compositional features of constituent minerals (2) suggest the possibility of a compositional difference of source magma between LZ-LCZ and UCZ-MZ-UZ. *i.e.*, Ca-poor Mg-rich magma for LZ-LCZ, and Ca-rich Mg-poor magma for UCZ-MZ-UZ. These two types of magmas are presumably identical with U (ultramafic) and A (anorthositic) magmas, respectively, as proposed by Irvine *et al.* (1983).

Compositional relationships of chromite summarized in (3) support an assumption for the crystallization process of LZ. At first, high Cr/(Al+Cr) chromite was formed, and enclosed by olivine. Then low Cr/(Al+Cr) chromite formed together with orthopyroxene in the matrix. In the CZ, high Cr/(Al+Cr) chromite probably formed prior to the plagioclase, and then plagioclase and orthopyroxene were formed later. There was re-equilibration between chromite and host mineral, although it could be ignored due to rapid cooling of the igneous intrusion. Thus the compositional variation of chromite seems to be in good agreement with the crystallization process.

6.2. Possible magma mixing

Taking the above inferred magma process into account, the rock exposed near the boundary between the LCZ and the UCZ is expected to record the magma mixing process. In the norite sample (0031705B2) collected from the UCZ, a poikilitic orthopyroxene developed-domain (Opx-rich domain) and a fine-grained clinopyroxene developed-domain (Cpx-rich domain) can be seen in the single thin section. Cumulus

plagioclase (An=69–75, Fe₂O₃=0.11–0.34 wt%, and MgO=0.01–0.03 wt%) occurs throughout the thin section, and is enclosed by orthopyroxene porphyroblast (X_{Mg} =75–76). Apart from the cumulus plagioclase, tiny rounded plagioclase (An=57, Fe₂O₃=0.88 wt%, and MgO=0.61 wt%) can be seen as inclusions. Fine clinopyroxene also includes tiny rounded plagioclase (An=77, Fe₂O₃=0.23–0.34, MgO=0.00–0.01 wt%) and orthopyroxene (X_{Mg} =77–80). The compositional difference of orthopyroxene probably implies that the orthopyroxene was crystallized from a different source, because both cumulus orthopyroxene and orthopyroxene inclusions have similar X_{Mg} ratios in the rock collected from different sequences (see Fig. 8). The plagioclase composition probably indicates the presence of two domains that contain high-An plagioclase (with low Fe₂O₃ and MgO) and low-An plagioclase (with high Fe₂O₃ and MgO) in an early stage. These two domains must be derived from two types of magmas, such as Ca-rich (Mg-poor) magma and Ca-poor (Mg-rich) magmas respectively. The former forms high-An plagioclase together with low X_{Mg} orthopyroxene and then clinopyroxene, whereas the latter forms low-An plagioclase at first, subsequently high-Mg poikilitic orthopyroxene. Eales *et al.* (1991) proposed a process of influx of magmatic liquid into the chamber, based on the composition of plagioclase inclusion within orthopyroxene and olivine in the LZ and CZ in the western Rustenburg Layered Suite. Compositional variations in relation to mineral texture, as observed here, support the magma mixing.

The sequence seems to consist mainly of normal fractionation from two types of magmas. However, previous work on continuous rock samples, *e.g.* borehole cores, has revealed multiple injection of magma, followed by mixing of new and resident magmas (Mitchell, 1990; Cawthorn *et al.*, 1991; Eales *et al.*, 1993). Eales *et al.* (1993) recognized several cyclic units in the LZ to UCZ on the basis of whole rock Mg/(Mg+Fe²⁺) ratios with higher values of several olivine cumulate layers. Cawthorn *et al.* (1991) suggest the addition of magma in the MZ and UZ, on the basis of Sr-isotopic study. Post-cumulus olivine in the harzburgite in the LZ (Fig. 4A), and reverse zoning of plagioclase in the UZ and MZ (Fig. 6), might be formed by the influx of primitive new Mg-rich magma and Ca-rich magma into pre-existent magma respectively. However, further discussion is needed, considering that a change in physical condition; for instance, changes the shape of the plagioclase phase diagram and “Constitutional supercooling” (Loomis, 1983).

In this paper, we reconfirm the crystallization sequence and presence of main two types of magmas from a small number of samples. Mineral texture and chemical compositions suggest the possibility of the magmas mixing in thin sections. Further study, for example, analyses of trace element abundance in each mineral (*e.g.* TiO₂ content in plagioclase) using SIMS, would contribute to understanding the magma mixing process in detail.

Acknowledgments

We thank Dr. G. Grantham for his arrangement of the field trip to the Rustenburg Layered Suite. S.B. sincerely thanks Dr. H.M. Rajesh for his English improvement and comment on the draft. Prof. H. Ishizuka, Dr. J. Maeda and an anonymous reviewer are thanked for their kind suggestions and constructive comments on earlier draft of the manuscript. S.B.’s research was supported by the “Japan Society for the Promotion of

Science". This study was supported by a Grant-in-Aid for General Scientific Research from the Japanese Ministry of Education, Science and Culture to K. Shiraishi (No. 09041116).

References

- Cameron, E.N. (1978): The lower zone of the eastern Bushveld Complex in the Olifants River trough. *J. Petrol.*, **19**, 437–462.
- Cameron, E.N. (1980): Evolution of the lower critical zone, central sector, eastern Bushveld Complex, and its chromite deposits. *Econ. Geol.*, **75**, 845–871.
- Cawthorn, R.G. and Davies, G. (1983): Experimental data on the parental magmas to the Bushveld Complex. *Contrib. Mineral. Petrol.*, **83**, 128–135.
- Cawthorn, R.G., Davies, G., Clubley-Armstrong, A.R. and McCarthy, T.S. (1981): Sills associated with the Bushveld Complex, South Africa: An estimate of the parental magma composition. *Lithos*, **14**, 1–15.
- Cawthorn, R.G., Meyer, P.S. and Kruger, F.J. (1991): Major addition of magma at the pyroxene marker in the Western Bushveld Complex, South Africa. *J. Petrol.*, **32**, 739–763.
- Davies, G., Cawthorn, R.G., Barton, J.M., Jr. and Morton, M. (1980): Parental magma to the Bushveld Complex. *Nature*, **287**, 33–35.
- Eales, H.V., Botha, W.J., Hattingh, P.J., De Klerk, W.J., Maier, W.D. and Odgers, A.T.R. (1993): The mafic rocks of the Bushveld Complex: a review of emplacement and crystallization history, and mineralization, in light of recent data. *J. Afr. Earth Sci.*, **16**, 121–142.
- Eales, H.V., Maier, W.D. and Teigler, B. (1991): Corroded plagioclase feldspar inclusions in orthopyroxene and olivine of the Lower and Critical Zones, Western Bushveld Complex. *Mineral. Mag.*, **55**, 63–80.
- Hall, A.L. (1932): The Bushveld Igneous Complex of the central Transvaal. *Geol. Surv. S. Afr. Mem.*, **28**, 560 p.
- Harmer, R.E. and Gittins, J. (1997): The origin of dolomitic carbonatites: field and experiment constrains. *J. Afr. Earth Sci.*, **25**, 5–28.
- Harmer, R.E. and Sharpe, M.R. (1985): Field relations and strontium isotope systematics of the marginal rocks of the eastern Bushveld Complex. *Econ. Geol.*, **80**, 813–817.
- Irvine, T.N. (1977): Chromite crystallization in the join Mg_2SiO_4 - $CaMgSi_2O_6$ - $MgCr_2O_4$ - SiO_2 . *Carnegie Inst. Washington Yearb.*, **76**, 465–472.
- Irvine, T.N., Keith, D.W. and Todd, S.G. (1983): The J.M. platinum-palladium reef of the Stillwater Complex, Montana: II. Origin by double-diffusive convection magma mixing and implications for the Bushveld Complex. *Econ. Geol.*, **78**, 1287–1334.
- Kretz, R. (1983): Symbols for rock-forming minerals. *Am. Mineral.*, **68**, 277–279.
- Kruger, P.J. (1992): The origine of the Merensky cyclic unit: Sr-isotope and mineralogical evidence for an alternative orthomagmatic model. *Aust. J. Earth Sci.*, **39**, 255–261.
- Lee, C.A. and Butcher, A.R. (1990): Cyclicity in the Sr-isotope stratigraphy through the Merensky and Bastard Reef Units, Atok Section, Eastern Bushveld Complex. *Econ. Geol.*, **85**, 877–883.
- Loomis, T.P. (1983): Compositional zoning of crystals: a record of Growth and Reaction History. *Kinetics and Equilibrium in Mineral Reactions*, ed. by S.K. Saxena. Berlin, Springer, 1–60.
- Mitchell, A.A. (1990): The stratigraphy, petrography and mineralogy of main zone of the northwestern Bushveld Complex. *S. Afr. J. Geol.*, **93**, 818–831.
- Sharpe, M.R. (1981): The chronology of magma influxes to the eastern compartment of the Bushveld Complex as exemplified by its marginal border groups. *J. Geol. Soc. London.*, **138**, 307–326.
- Sharpe, M.R. and Irvine, T.N. (1983): Melting relations of two Bushveld chilled margin rocks and implications for the origin of chromite. *Carnegie Inst. Washington Yearb.*, **82**, 295–300.
- Tankard, A.J., Jackson, M.P.A., Eriksson, K.A., Hobday, D.K., Hunter, D.R. and Minter, W.E.L. (1982): *Crustal Evolution of Southern Africa, 3.8 Billion Years of Earth History*. Heidelberg, Springer, 523 p.
- Togashi, S., Kita, N.T., Tomiya, A. and Morishita, Y. (1998): Ion Microprobe (ims 1270) Quantitative

- analysis of trace element of volcanic plagioclase using high mass resolution method. *Eos, Trans. AGU*, **79**, 45, F951.
- Von Gruenewaldt, G. (1973): The main and upper zones of the Bushveld Complex in the Roosenekal area, eastern Transvaal. *Geol. Soc. S. Afr. Trans.*, **76**, 56–61.
- Von Gruenewaldt, G., Sharpe, M.R. and Hatton, C.J. (1985): The Bushveld Complex: Introduction and Review. *Econ. Geol.*, **80**, 803–812.
- Wager, L.W. and Brown, G.M. (1968): *Layered Igneous Rocks*. Edinburgh, Oliver and Boyd, 588 p.
- Wallmach, T., Eriksson, P.G., Hatton, C.J., Harmer, R.E., Schweitzer, J.K. and Reczko, B.F.F. (1995): *Geocongress '95, Bushveld Kaleidoscope-Excursion Guidebook*. Pretoria, University of Pretoria, 29 p.
- Wilson, M. (1989): *Igneous Petrogenesis*. London, Chapman & Hall, 466 p.

(Received December 27, 2000; Revised manuscript accepted May 15, 2001)